Synthesis of bifunctionalized-pore mesoporous organosilica. Study of the accessibility and the distribution of functions in the pore channels

Rola Mouawia, Ahmad Mehdi,* Catherine Reyé and Robert Corriu*

Received (in Montpellier, France) 8th March 2006, Accepted 22nd May 2006
First published as an Advance Article on the web 7th June 2006
DOI: 10.1039/b603530b

In this paper, we report the synthesis in one step of ordered (hexagonal phase) mesoporous silicas functionalized with two different organic groups [$HS(CH_2)_3$– and acac$(CH_2)_3$–] located in the pore channels. These materials were characterized by X-ray diffraction measurements, transmission electron spectroscopy, nitrogen adsorption analyses and solid state ^{13}C and ^{29}Si NMR spectroscopies. The bifunctionalization of the internal pore's surface by the organic groups was clearly evidenced by elemental analyses and chemical reactivity. In addition, we have shown that the organic groups were regularly distributed on the pore's surface.

Introduction

Since the discovery of ordered mesoporous silica,[1] many research efforts have been directed towards the modification of the inner pore surface of mesoporous materials. To this end, post-synthesis grafting of an organotrialkoxysilane $RSi(OR')_3$ onto the pore surface of the silica was often used.[2] However, this method does not allow control of the loading or the distribution of the functional groups.[3] A one step alternative approach, overcoming the main restrictions of the post-synthesis method, has been developed.[4–8] It consists of the copolymerisation of tetraethylorthosilicate (TEOS) and an organotrialkoxysilane $RSi(OR')_3$ in the presence of a structure-directing agent. This method requires that the R group be sufficiently hydrophobic to enter the core of the micelle and not too bulky to avoid its perturbation. A large variety of functional groups have been incorporated into mesoporous materials by this route. The introduction of two distinct organic groups into the channel pores was also considered but gave rise to a number of much more limited studies. Mann *et al.*[9] reported the first direct synthesis of bifunctional mesoporous materials using mercaptopropyltriethoxysilane (MPTES) and 3-aminopropyltriethoxysilane (APTES) as precursors and cetyl trimethyl ammonium bromide (CTAB) as surfactant. The same year, Macquarrie[10] synthesized a bifunctional material with APTES and phenyl groups and showed the positive effect of the incorporation of the non-polar phenyl groups on the catalytic activity of the material. Stucky *et al.*[11] reported the preparation of an ordered functionalized mesoporous silica containing sulfonic acid groups and non-polar organic moieties (methyl or benzyl) using Pluronic 123 (P123) as surfactant. They examined whether the presence of the second functional group influenced the strength of the sulfonic acid centers or not by ^{31}P MAS-NMR spectroscopy. However, the changes observed in the ^{31}P NMR spectra did not give any evidence on the distribution of the two functional groups (segregation or uniform distribution). Recently, Lin *et al.*[12] described a new method allowing not only the introduction of two organic groups in mesoporous silica but also the control of the particle size and shape of the resulting material. Finally, bifunctionalization of the channel pores in two steps, that is introduction of the first function by direct synthesis followed by a post-synthesis reaction to introduce the second one, have been exploited by several research groups.[13–15] However, in all cases, the question on segregation or regular distribution of the functional groups on the pore surface remained unsolved. This important question prompted us to investigate the accessibility and distribution of two distinct organic groups incorporated within the channel pores of mesoporous silica. The following groups were selected for that purpose: acetylacetonato (acac) propyl (precursor **1**) and 3-mercaptopropyl (precursor **2**).

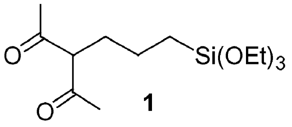
1

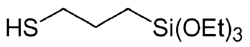
2

In this paper, we report the preparation and characterization of mesoporous silicas with mono and bifunctionalized pores. The ability of the acac groups to complex lanthanides and the ion-exchange capacity of the SO_3H groups have been exploited to elucidate the distribution of these functions on the pore surface, first on monofunctional materials (using either **1** or **2**), then on bifunctional materials (using both **1** and **2**). We show that both functional groups were regularly distributed on the pore surface of the bifunctional materials.

Experimental

General procedures

Triblock copolymer ($EO_{20}PO_{70}EO_{20}$ with PEO = poly(ethylene oxide) and PPO = poly(propylene oxide)), Pluronic 123, 3-mercaptopropyltriethoxysilane (**2**), tetraethylorthosilicate (TEOS), acetylacetone, potassium *tert*-butoxide, sodium

---

Chimie Moléculaire et Organisation du Solide, UMR 5637 CNRS, Institut Charles Gerhardt, Université Montpellier II, Sciences et Techniques, Place E. Bataillon, F-34095 Montpellier Cedex 5, France. E-mail: ahmad.mehdi@univ-montp2.fr; Fax: +33 4 6714 3852; Tel: +33 4 6714 3038

fluoride (NaF) and $EuCl_3 \cdot 6H_2O$ salt were purchased from Aldrich and used as supplied. 3-Iodopropyltriethoxysilane was prepared by halogen exchange reaction between 3-chloropropyltriethoxysilane and NaI according to the procedure previously described.[16] The ^{29}Si CP-MAS solid state NMR spectra and ^{13}C CP-MAS solid state NMR spectra were recorded on a BRUKER FTAM 300, in the latter case by using the TOSS technique. In both cases, the repetition time was 5 and 10 s with contact times of 5 and 2 ms. Specific surface areas were determined by the Brunauer–Emmett–Teller (BET) method on a Micromeritics ASAP 2010 analyser (using 74 points and starting from 0.01 as the value for the relative pressure) and the average pore diameters were calculated by the BJH method. Powder X-ray diffraction patterns were measured on a Bruker D5000 diffractometer equipped with a rotating anode (Institut Européen des Membranes, UMR ENSCM-UMII-CNRS 5625, Montpellier, France). Transmission electron microscopy (TEM) observations were carried out at 100 kV on a JEOL 1200 EXII microscope. Samples for TEM measurements were prepared using ultramicrotomy techniques and were then deposited on copper grids. Elemental analyses were performed by the Service Central d'Analyse (CNRS, Vernaison, France).

Syntheses

$[CH_3C(O)]_2CH(CH_2)_3Si(OCH_2CH_3)_3$, 1. **1** was obtained with 70% yield according to the procedure previously described.[17]

SBA-$^{x}\Sigma$ (x = 5, 10 and 14). All the materials SBA-$^{x}\Sigma$ were prepared according to the same procedure. The preparation of SBA-^{10}acac is given as an example.

SBA-^{10}acac. 4.0 g of P123 ($EO_{20}PO_{70}EO_{20}$) were dissolved in an aqueous HCl solution (160 mL, pH $\approx$ 1.5). This solution was poured on a mixture of TEOS (8.41 g, 40.4 mmol) and **1** (1.33 g, 4.4 mmol) at ambient temperature. The molar composition of the reaction mixture was: $0.04F^- : 1TEOS : 0.11\mathbf{1} : 0.02P123 : 0.12HCl : 220H_2O$. The mixture was stirred for 30 min giving rise to a microemulsion. After heating this perfectly transparent solution at 60 °C, a small amount of NaF (80 mg) was added under stirring to induce polycondensation. The mixture was left at 60 °C under stirring for 48 h. The resulting solid was filtered and washed with ethanol. The surfactant was removed by hot ethanol extraction in a Soxhlet apparatus over 24 h. After filtration and drying at 50 °C under vacuum, 2.9 g (3.9 mmol, 87%) of SBA-^{10}acac were obtained as a white solid.

SBA-^{5}acac. Starting from TEOS (8.86 g, 42.6 mmol) and **1** (0.66 g, 2.2 mmol). 2.69 g (92%) of SBA-^{5}acac were obtained as a white powder.

SBA-^{14}acac. Starting from TEOS (7.99 g, 38.4 mmol) and **1** (1.96 g, 6.4 mmol). 2.94 g (83%) of SBA-^{14}acac were obtained as a white powder.

SBA-^{5}SH. Starting from TEOS (8.86 g, 42.6 mmol) and **2** (0.52 g, 2.2 mmol). 2.67 g (96%) of SBA-^{5}SH were obtained as a white powder.

SBA-^{10}SH. Starting from TEOS (8.41 g, 40.4 mmol) and **2** (1.04 g, 4.4 mmol). 2.64 g (96%) of SBA-^{10}SH were obtained as a white powder.

SBA-^{14}SH. Starting from TEOS (7.99 g, 38.4 mmol) and **2** (1.51 g, 6.4 mmol). 2.70 g (87%) of SBA-^{14}SH were obtained as a white powder.

SBA-^{14}acac,SH. Starting from TEOS (8.41 g, 40.4 mmol), **1** (0.98 g, 3.2 mmol) and **2** (0.75 g, 3.2 mmol). 2.82 g (85%) of SBA-^{14}acac,SH were obtained as a white powder.

Results and discussion

Preparation and characterization of ordered monofunctional mesoporous silica

Firstly, we prepared SBA-15 mesoporous silicas containing a variable amount of thiol (SH) or acetylacetonate (acac) units. The synthesis of these monofunctional silicas was achieved by copolymerisation of acetylacetonatopropyltriethoxysilane[17] **1** or 3-mercaptopropyltriethoxysilane **2** and TEOS in the presence of P123 as structure-directing agent (Scheme 1). The surfactant was removed from the as-synthesized material by Soxhlet extraction with refluxing ethanol for 24 h to give the functionalized materials denoted SBA-$^{x}\Sigma$ [SBA recalls here the surfactant used (P123), Σ specifies the presence of functional groups (SH or acac) inside the pore channels and x indicates the molar% of organic group in the initial mixture (5, 10 and 14%)]. The composition of the final materials was inferred from the results of Si, C and S elemental analysis. They were found to be close to those for the original mixtures as indicated in Table 1.

Powder X-ray diffraction patterns of different samples (Fig. 1) exhibited an intense diffraction peak corresponding to the d_{100} spacing. Although no reflections higher than d_{100} have been clearly resolved, Pinnavaia *et al.* have shown that similar single reflection materials can still exhibit local hexagonal symmetry.[18] The identification of the first Bragg peak as the reflection from the (100) scattering planes of the hexagonal structure allows determination of the hexagonal lattice parameter a_0 (see Table 1).

Further evidence for a highly ordered hexagonal structure was provided by transmission electron microscopy (TEM) micrographs, as shown in Fig. 2.

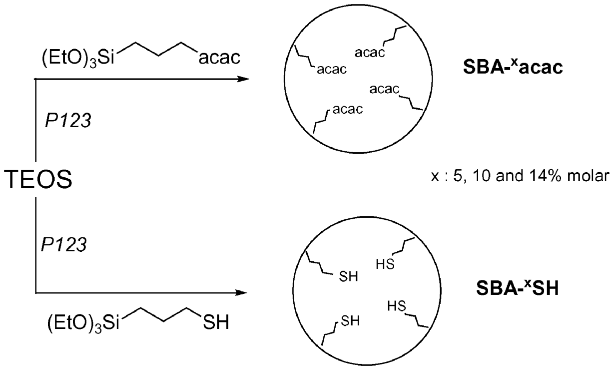

Scheme 1 Preparation of SBA-^{x}acac and SBA-^{x}SH materials.

Table 1 Physicochemical characteristics of functionalized mesoporous silica

	SBA-^{5}acac	SBA-^{10}acac	SBA-^{14}acac	SBA-^{5}SH	SBA-^{10}SH	SBA-^{14}SH	SBA-^{14}acac,SH
S_{BET}/m^2 g^{-1}	763	675	600	669	583	569	792
V_p/cm^3 g^{-1}	1.28	1.04	0.7	0.9	0.58	0.44	092
$D_p{}^a$/Å	74.4	68.7	62.5	52.6	38.5	32	45.8
d_{100}/Å	129	115	80	119	95	88	103
a_0/Å	149	133	92	138	109	102	
Wall thickness/Å	74.6	64.3	29.5	85.4	70.5	70	73.2
Organic group content^b/mmol g^{-1}	0.71 (0.75)	1.30 (1.36)	1.70 (1.80)	0.74 (0.79)	1.30 (1.49)	1.92 (2.0)	1.76^c (1.90)

[a] Calculated from the desorption branch by using the BJH method. [b] Calculated from elemental analysis (theoretical values). [c] 0.9 acac and 0.86 SH.

The N_2 adsorption–desorption isotherms of materials SBA-$^x\Sigma$ are type IV, characteristic of mesoporous materials with a narrow pore size distribution (Fig. 3). The textural data of the materials are given in Table 1. It is worth noting that the surface area (S_{BET}), pore volumes (V_p) and mean pore diameters (D_p) of these materials are large, the mean pore diameters increasing as the loading of organic groups decreased.

The incorporation of organic groups in the mesoporous materials and the removal of surfactant were confirmed by solid state NMR spectroscopies. ^{13}C CP-MAS NMR spectra of SBA-^{10}acac and SBA-^{10}SH revealed that the organic groups remained intact as shown by the signals at 26.5 ppm (resonance of SH–CH_2), 205.4 ppm (carbonyl resonances) and the three additional signals (14.0, 20.9 and 28.7 ppm) attributed to the propyl spacer. A typical ^{29}Si CP-MAS NMR spectrum displayed signals at −101.89 ppm and −111.60 ppm, attributed to Q^3 and Q^4 substructures respectively, denoting high cross-linking of the species. An additional signal at −66.75 ppm assigned to T^3 substructure revealed fully cross-linked organosilsesquioxane species.

Oxidation of SH group into SO_3H was achieved by treating samples SBA-^{x}SH with a H_2O_2 solution (300 equivalents) at room temperature for 2 h, followed by a diluted sulfuric acid solution for 30 min. The quantitative transformation of SH group into SO_3H in the resulting SBA-^{x}SO_3H materials was evidenced by X-ray photoelectron spectroscopy (XPS).

Powder X-ray diffraction patterns of different samples SBA-^{x}SO_3H were very similar to those of the starting materials. They exhibited a diffraction peak corresponding to the d_{100} spacing, indicating that the hexagonal structure was maintained.

Complexation of Eu^{III} by acetylacetonate moieties within the materials SBA-^{x}acac

The complexation of $EuCl_3$ by the acac moieties located inside the pore channels of materials SBA-^{x}acac was investigated in order to study the accessibility and distribution of these groups. The materials SBA-^{x}acac were treated with an excess of $EuCl_3 \cdot 6H_2O$ (2 equiv. of Eu^{III} per acac moiety) in ethanol heated under reflux for 12 h (Scheme 2). The resulting solids, named SBA-^{x}acac,Eu, were copiously washed with hot ethanol in order to eliminate any non-complexed salt. The filtrate containing the excess of $EuCl_3$ salt was titrated by complexometry measurements. The uptake of Eu^{III} ions per g of material was inferred from the titration measurements. It was found to be highly dependent on the composition of the materials, that is on the molar% of acac groups present in the

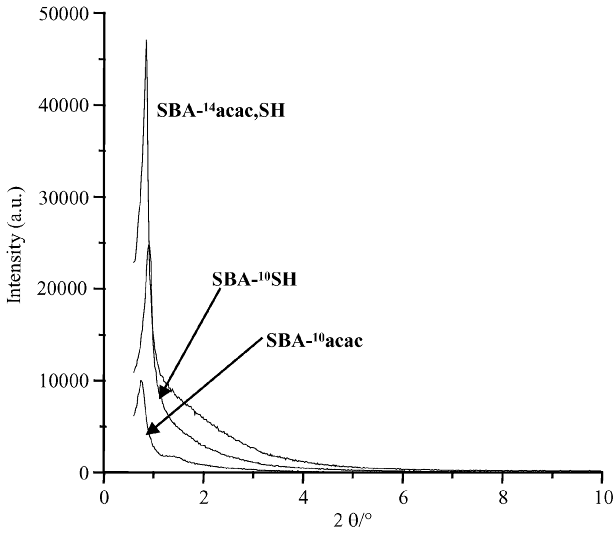

Fig. 1 XRD patterns of SBA-^{10}acac, SBA-^{10}SH and SBA-^{14}acac,SH.

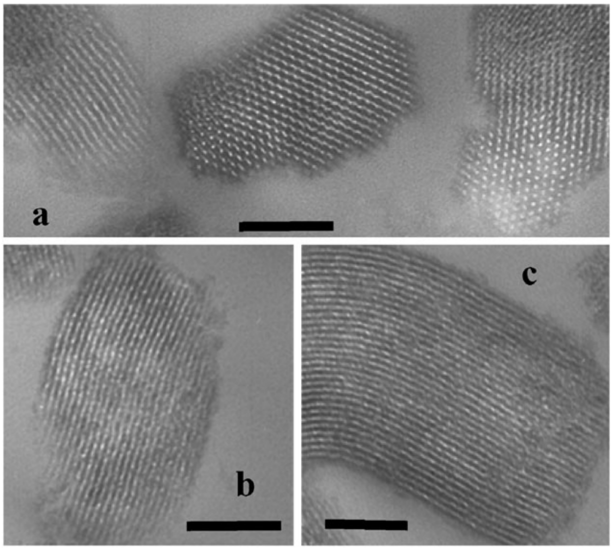

Fig. 2 TEM micrographs of SBA-^{10}acac (a), SBA-^{10}SH (b) and SBA-^{14}acac,SH (c). Scale bars = 100 nm.

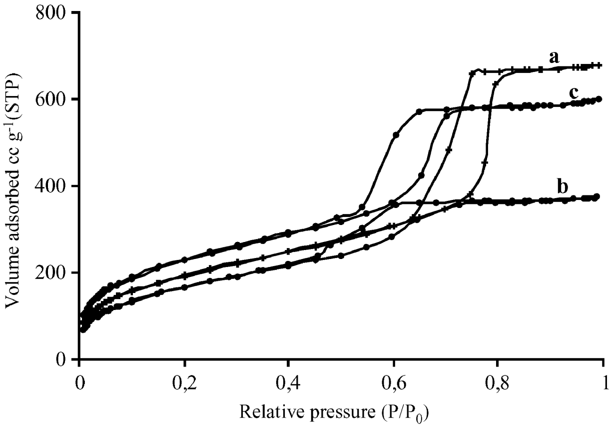

Fig. 3 Nitrogen adsorption–desorption isotherms of SBA-^{10}acac (a), SBA-^{10}SH (b) and SBA-^{14}acac,SH (c).

pore channels. The ratio of Eu : acac moieties was then deduced from both the titration and the materials' compositions (Table 2). Results of elemental analyses of Eu, Cl and C gave rise to exactly the same Eu : acac ratio as the ones found by titration (Table 2). In the case of SBA-^{14}acac,Eu, the Eu : acac ratio was found to be exactly 0.5, indicating that at this concentration, two acac groups are sufficient to coordinate one europium ion. Thus, in this material, all the acac units are accessible and used in the complexation reaction. It is worth noting that the Eu^{III} uptake due to only two acac moieties in the pore channels is a particularly remarkable result, considering that lanthanide complexes exhibit coordination numbers ranging from six to twelve (in the solid state and in solution), with eight and nine being the most commonly observed.[19]

When the concentration of acac groups decreases, the Eu : acac ratio decreases dramatically. It was found to be 0.035 for SBA-^{10}acac,Eu and 0 for SBA-^{5}acac,Eu. This drop is believed to result from the increasing distance between the acac units, as the acac concentration decreases (in SBA-^{10}acac and SBA-^{5}acac) thus forbidding additional Eu^{III} uptake (Scheme 3). The number of functional groups per nm^2 can be deduced from the results of elemental analyses and the values of the BET surface area. It was found to be 1.70, 1.16 and 0.56 acac/nm^2 for x = 14, 10 and 5, respectively (Table 2).

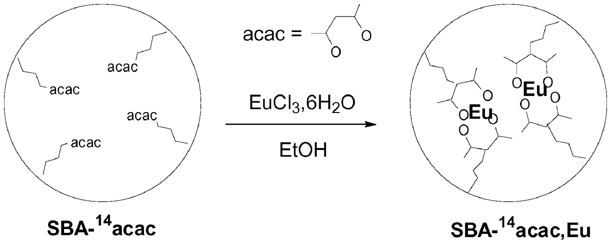

Scheme 2 Complexation of europium chloride by acetylacetone units.

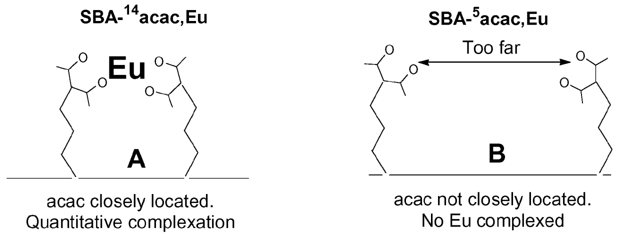

Scheme 3 Schematic representation of the organic groups on the pore surface in SBA-^{14}acac,Eu (A) and SBA-^{5}acac,Eu (B).

Finally, the dramatic drop in Eu^{III} uptake as the number of acac groups decreases is a good indicator of their regular distribution in the pore channels.

Ion-exchange capacities of the sulfonic acid moieties within the materials SBA-$^{x}SO_3H$

In order to elucidate the distribution of the sulfonic acid groups on the surface of the pore channels, we used the ion-exchange reaction between the sulfonic acid groups of SBA-$^{x}SO_3H$ samples and NaCl. Indeed, it is known that acidic or basic moieties confined to a surface may exhibit a reactivity significantly different from the one they possess in dilute solution.[20] The ion-exchange reaction was achieved by treating SBA-$^{x}SO_3H$ with an aqueous solution of sodium chloride (NaCl, 2 M) at room temperature for 1 h (Scheme 4). The resulting solids, named SBA-$^{x}SO_3Na$, were washed with water. The filtrate containing the generated HCl was colorimetrically titrated by sodium hydroxide solution (NaOH, 0.01 N). The ion-exchange capacity of SO_3H groups was calculated from the titration measurements (Table 2). It was found to be incomplete for the SBA-$^{14}SO_3H$ (57%). The ion-exchange capacity increased to become 65% for SBA-$^{10}SO_3H$ while it was quantitative for SBA-$^{5}SO_3H$. The changes in the acid character of the SO_3H groups in our materials can be explained by the corresponding changes in the proximity of the SO_3H moieties on the pore's surface. In the SBA-$^{14}SO_3H$

Table 2 Physicochemical characteristics of functionalized mesoporous silica

Materials	Organic units[a] per nm^2	Eu : acac ratio[d]	Complexation[e] (%)	Exchange[f] (%)
SBA-^{5}acac,Eu	0.56[b]	0 (0)	0	—
SBA-^{10}acac,Eu	1.16[b]	0.035 (0.04)	10	—
SBA-^{14}acac,Eu	1.70[b]	0.50 (0.52)	100	—
SBA-$^{5}SO_3H$	0.66[c]	—	—	100
SBA-$^{10}SO_3H$	1.34[c]	—	—	65
SBA-$^{14}SO_3H$	2.03[c]	—	—	57
SBA-^{14}acac,Eu,SH	0.68[b] and 0.65[c]	0 (0)	0	—
SBA-^{14}acac,SO_3H	0.68[b] and 0.65[c]	—	—	100

[a] Estimated from the elemental analysis and the BET surface area. [b] Values for acac units. [c] Values for SH or SO_3H units. [d] Calculated from the elemental analysis (complexometry measurements). [e] Considering that 2 acac are needed for 1 Eu. [f] From titration measurements.

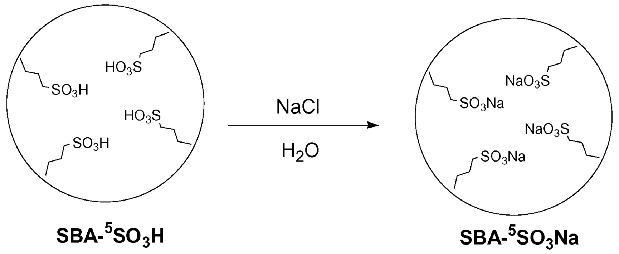

Scheme 4 Exchange reaction between NaCl and sulfonic acid groups.

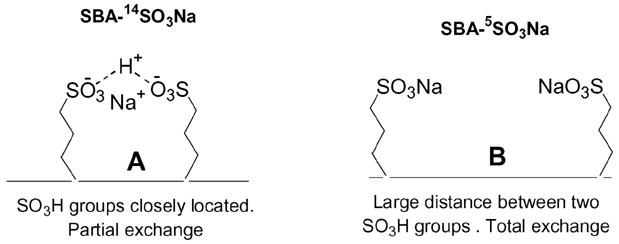

Scheme 5 Schematic representation of the sulfonic salt groups on the pore surface in SBA-$^{14}SO_3Na$ (A) and SBA-$^5SO_3Na$ (B).

material, the observed partial exchange is attributed to the stabilization of non-ionized groups by adjacent ionized groups (Scheme 5A), which prevents the ion-exchange reaction from occurring. This should be due to the high number of sulfonic acid groups (2.03 SO_3H per nm^2) on the pore's surface, which should be in close proximity[20] to each other in this material. In contrast, in SBA-$^5SO_3H$, the SO_3H groups react as strong acids, as in a dilute solution situation. This means that the SO_3H groups must be sufficiently isolated (0.66 SO_3H per nm^2) (Scheme 5B) to behave independently from each other. Therefore, the exchange reaction becomes complete. The situation for SBA-$^{10}SO_3H$ is just in between that of SBA-$^{14}SO_3H$ and SBA-$^5SO_3H$.

Here again, it is worth noting that the dramatic increase in the rate of ion-exchange as the concentration of SO_3H decreases is a good indicator of the regular distribution of SO_3H groups on the pore's surface.

Distribution of functional groups within the pores of bifunctionalized materials

For this study, we synthesised a material containing both acac and SH groups by the one-pot method. The synthesis of this bifunctional material was achieved by copolymerisation of a ternary mixture containing precursors **1** and **2** and TEOS in the presence of P123 as structure-directing agent (Scheme 6). An equimolar content of **1** (7%) and **2** (7%) was introduced in the original mixture, the total organic content being 14 molar%. The composition of the resulting material, which was named SBA-^{14}acac,SH was inferred from the results of elemental analysis of Si, C and S. It was found to be close to that of the original mixture, as indicated in Table 1, with a molar content of SH groups almost equal to that of acac groups.

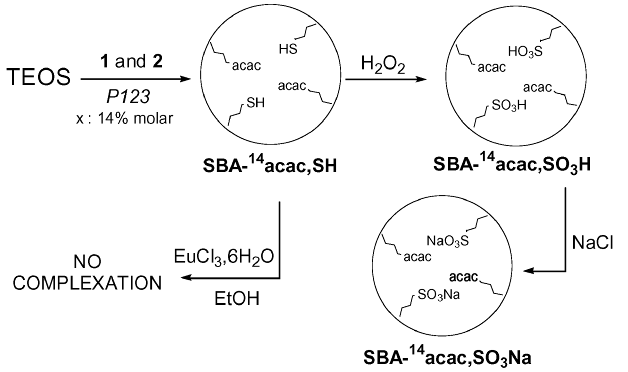

Scheme 6 Preparation and chemical transformation of SBA-^{14}acac, SH material containing acac and SH groups on the pore surface.

The powder X-ray diffraction pattern for SBA-^{14}acac,SH (Fig. 1) exhibited an intense diffraction peak corresponding to the d_{100} spacing (Table 1). The TEM micrograph of an SBA-^{14}acac,SH sample presented in Fig. 2 clearly shows a highly ordered hexagonal structure.

The N_2 adsorption–desorption isotherm of SBA-^{14}acac,SH is type IV, characteristic of mesoporous materials with a narrow pore size distribution (Fig. 3). The textural data for SBA-^{14}acac,SH are given also in Table 1.

Oxidation of the SH group into SO_3H was achieved as previously described (*vide supra*) resulting in the corresponding SBA-^{14}acac,SO_3H material. The XPS data revealed a quantitative transformation of SH groups into SO_3H.

In order to elucidate the distribution of the organic units in SBA-^{14}acac,SO_3H, we studied both the $EuCl_3$ salt uptake and the ion-exchange reaction with NaCl.

SBA-^{14}acac,SO_3H was treated with an excess of $EuCl_3$, $6H_2O$ (2 equiv. of Eu^{III} per acac moiety) in ethanol heated under reflux for 12 h (Scheme 6). The resulting solid, named SBA-^{14}acac,Eu,SO_3H, was copiously washed with hot ethanol in order to eliminate any excess of salt. The filtrate was titrated by complexometry measurements. It was found that there was no Eu^{III} uptake within this material (Table 2). This result

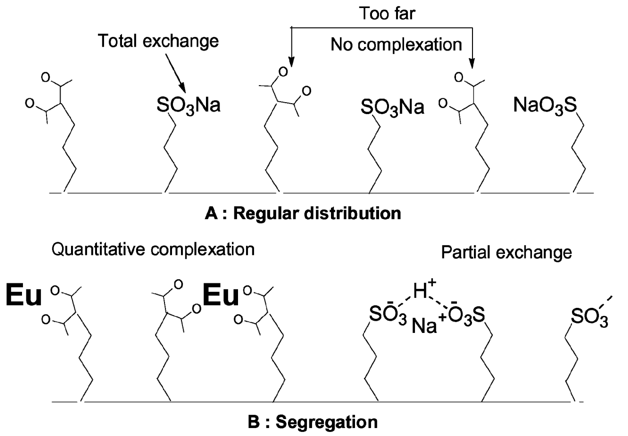

Scheme 7 Schematic representations of the bifunctionalized surface in SBA-^{14}acac,SO_3H. With regular distribution (A) or segregation (B) of organic units.

indicates that in SBA-^{14}acac,SO_3H the acac units are not in close proximity to each other, thus preventing the Eu^{III} uptake from occurring. In another experiment, treatment of SBA-^{14}acac,SO_3H with an aqueous solution of sodium chloride (NaCl, 2 M) at room temperature for 1 h (Scheme 6) and filtration gave rise to a material named SBA-^{14}acac,SO_3Na. The colorimetric titration revealed that the ion-exchange capacity of SO_3H groups in this sample was total (Table 2). This indicates that the SO_3H groups were sufficiently isolated from each other to behave as strong acids in the material.

These two results are very similar to those obtained for SBA-$^5SO_3H$ and SBA-^{5}acac and are in agreement with a uniform distribution of SO_3H and acac groups in the pore channels at this concentration (Scheme 7A). Indeed, if the groups had been introduced with segregation (Scheme 7B), the ion-exchange capability of the SO_3H groups would have been only partial as in SBA-$^{14}SO_3H$ and the Eu^{III} uptake would have been quantitative as observed for SBA-^{14}acac.

Conclusions

We have demonstrated that the one-pot synthesis of a mesoporous silica with equal amounts of acetylacetonate and mercapto groups in the pore channels gave rise to a material which exhibited the same hexagonal symmetry phase as those observed for the corresponding monofunctionalized materials. By using their respective reactivities, coordination abilities and ion-exchange, we have been able to conclude unambiguously that these groups were regularly distributed on the surface of the pore channels of the resulting bifunctional material. Both groups can be considered as moderately polar. This interesting result incites us to study the distribution of other binary mixtures in order to clear some rules.

Acknowledgements

The authors thank Dr Arie van der Lee (IEM, UMR 5635 Montpellier, France) for XRD measurements, the CNRS and the Université Montpellier II for financial support.

References

1 (*a*) C. T. Kresge, M. E. Leonowicz, W. J. Roth, J. C. Vartuli and J. S. Beck, *Nature*, 1992, **359**, 710; (*b*) J. S. Beck, J. C. Vartuli, W. J. Roth, M. E. Leonowicz, C. T. Kresge, K. D. Schmitt, C. T.-W. Chu, D. H. Olson, E. W. Sheppard, J. B. McCullen, J. B. Higgins and J. L. Schlenker, *J. Am. Chem. Soc.*, 1992, **114**, 10834.

2 (*a*) W. Zhang, M. Froba, J. Wang, P. T. Tanev, J. Wong and T. J. Pinnavaia, *J. Am. Chem. Soc.*, 1996, **118**, 9164; (*b*) L. Mercier and T. J. Pinnavaia, *Adv. Mater.*, 1997, **9**, 500; (*c*) A. Cauvel, G. Renard and D. Brunel, *J. Org. Chem.*, 1997, **62**, 749; (*d*) P. M. Price, J. H. Clark and D. J. Macquarrie, *J. Chem. Soc., Dalton Trans.*, 2000, 101.

3 (*a*) D. J. Macquarrie, D. B. Jackson, J. E. J. Mdoe and J. H. Clark, *New J. Chem.*, 1999, **23**, 539; (*b*) A. Walcarius and C. Delacôte, *Chem. Mater.*, 2003, **15**, 4181.

4 S. L. Burkett, S. D. Sims and S. Mann, *Chem. Commun.*, 1996, 1367.

5 D. J. Macquarrie, *Chem. Commun.*, 1996, 1961.

6 D. J. Macquarrie, D. B. Jackson, S. Tailland and K. A. Utting, *J. Mater. Chem.*, 2001, **11**, 1843.

7 Y. Mori and T. J. Pinnavaia, *Chem. Mater.*, 2001, **13**, 2173.

8 (*a*) R. J. P. Corriu, C. Hoarau, A. Mehdi and C. Reye, *Chem. Commun.*, 2000, 71; (*b*) R. J. P. Corriu, F. Embert, Y. Guari, A. Mehdi and C. Reye, *Chem. Commun.*, 2001, 1116.

9 S. R. Hall, C. E. Fowler, B. Lebeau and S. Mann, *Chem. Commun.*, 1999, 201.

10 D. J. Macquarrie, *Green Chem.*, 1999, **1**, 195.

11 D. Margolese, J. A. Melero, S. C. Christiansen, B. F. Chmelka and G. D. Stucky, *Chem. Mater.*, 2000, **12**, 2448.

12 S. Huh, H.-T. Chen, J. W. Wiench, M. Priski and V. S.-Y. Lin, *J. Am. Chem. Soc.*, 2004, **126**, 1010.

13 E. Cano-Serrano, G. Blanco-Brieva, J. M. Campos-Martin and J. L. G. Fieorro, *Langmuir*, 2003, **19**, 7621.

14 W.-H. Zhang, X.-B. Lu, J.-H. Xiu, Z.-L. Hua, L.-X. Zhang, M. Robertson, J.-L. Shi, D.-S. Yan and J. D. Holmes, *Adv. Funct. Mater.*, 2004, **14**, 544.

15 F. Goettmann, D. Grosso, F. Mercier, F. Mathey and C. Sanchez, *Chem. Commun.*, 2005, 1240.

16 E. Besson, A. Mehdi, D. Lerner, C. Reyé and R. J. P. Corriu, *J. Mater. Chem.*, 2005, **15**, 803.

17 V. Matsura, Y. Guari, J. Larionova, C. Guerin, A. Caneschi, C. Sangregorio, E. Lancelle-Beltran, A. Mehdi and R. J. P. Corriu, *J. Mater. Chem.*, 2004, **14**, 3026.

18 (*a*) P. T. Tanev and T. J. Pinnavaia, *Science*, 1995, **267**, 865; (*b*) P. T. Tanev, M. Chibwe and T. J. Pinnavaia, *Nature*, 1994, **368**, 321.

19 F. S. Richardson, *Chem. Rev.*, 1982, **82**, 541.

20 J. J. Shyue, M. R. De Guire, T. Nakanishi, Y. Masuda, K. Koumoto and C. N. Sukenik, *Langmuir*, 2004, **20**, 8693.